

# The Design and Fabrication of One-dimensional Random Surfaces with Specified Scattering Properties

© T.A. Leskova, A.A. Maradudin\*, E.R. Méndez\*\*, A.V. Shchegrov\*\*\*

Institute of Spectroscopy of Russian Academy of Sciences,  
142092 Troitsk, Moscow region, Russia

\* Department of Physics and Astronomy and Institute for Surface and Interface Science University of California,  
Irvine CA 92697 USA

\*\* División de Física Aplicada Centro de Investigación Científica y de Educación Superior de Ensenada Apdo. Postal 2732  
22800 Ensenada, B.C. México

\*\*\* Rochester Theory Center for Optical Science and Engineering Department of Physics and Astronomy  
University of Rochester  
Rochester, NY 14627 USA

E-mail: aamaradu@usi.edu

We describe methods for designing and fabricating one-dimensional random surfaces that scatter light uniformly within a specified range of scattering angles, and produce no scattering outside this range. These methods are tested by means of computer simulations, and preliminary experimental results are presented.

The first theoretical study of the scattering of light from a randomly rough surface was published by Mandel'shtam in 1913, in the context of the scattering of light from a liquid surface [1]. In the succeeding years the overwhelming majority of the theoretical work in this field has continued to be devoted to the solution of such direct problems, namely given the statistical properties of a random surface, to calculate the angular and polarization dependence of the intensity of the scattered light. In contrast, in this paper we study theoretically and experimentally an inverse problem in rough surface scattering, namely the design and fabrication of a random surface that scatters light in a prescribed way.

For many practical applications it is desirable to have optical elements whose light scattering properties can be controlled. In particular, a non-absorbing diffuser that scatters light uniformly within a specified range of scattering angles, and produces no scattering outside this range, would have applications, for example, to projection systems, where it is important to produce even illumination without wasting light. We will call such an element a band-limited uniform diffuser.

The design of uniform diffusers has been considered by several authors. The case of binary diffusers has been studied by Kurtz [2], and work on special cases of one-dimensional diffusers has been reported by Kurtz et al. [3] and by Nakayama and Kato [4]. Some work on the more general two-dimensional case has been carried out by Kowalczyk [5]. In addition, diffractive optical elements that scatter light uniformly throughout specified angular regions have recently become commercially available. These elements, however, are not truly random, and possess the desired characteristics over only a relatively narrow range of wavelengths.

Despite the interest in the problem, at the present time there are no clear procedures for designing and fabricating random, band-limited uniform diffusers, and it is unclear what kind of statistics are required for the production of such an optical element. In this paper, that extends earlier work

by the authors [6,7], we address these questions for the case of one-dimensional diffusers. We illustrate the ideas involved by considering the scattering of *s*-polarized light from a one-dimensional, randomly rough, perfectly conducting surface. By working within the Kirchhoff approximation, and motivating the approach by taking the geometrical optics limit of this approximation, we describe methods for designing and fabricating achromatic, random, uniform diffusers of light, and test these methods by computer simulations and experimentally.

## 1. Light Scattering in the Geometrical Optics Limit of the Kirchhoff Approximation

To motivate the calculations that follow we begin by considering the scattering of *s*-polarized light from a one-dimensional, randomly rough, perfectly conducting surface defined by  $x_3 = \zeta(x_1)$ . The region  $x_3 > \zeta(x_1)$  is vacuum, the region  $x_3 < \zeta(x_1)$  is the perfect conductor. The plane of incidence is the  $x_1x_3$ -plane. The surface profile function  $\zeta(x_1)$  is assumed to be a differentiable, single-valued function of  $x_1$ , and to constitute a random process, but not necessarily a stationary one.

The surface is illuminated from the vacuum region. The single nonzero component of the total electric field in this region is the sum of an incident wave and of the scattered field

$$E_2(x_1, x_3 | \omega) = \exp[ikx_1 - i\alpha_0(k)x_3] + \int_{-\infty}^{\infty} \frac{dq}{2\pi} R(q|k) \exp[iqx_1 + i\alpha_0(q)x_3], \quad (1.1)$$

where  $\alpha_0(q) = [(\omega/c)^2 - q^2]^{1/2}$ ,  $\text{Re } \alpha_0(q) > 0$ ,  $\text{Im } \alpha_0(q) > 0$ , and  $\omega$  is the frequency of the incident light. A time dependence of the form of  $\exp(-i\omega t)$  is assumed, but explicit reference to it is suppressed.

In the Kirchhoff approximation, which we adopt here for simplicity, the scattering amplitude  $R(q|k)$  is given by

$$R(q|k) = \frac{-i}{2\alpha_0(q)} \times \int_{-\infty}^{\infty} dx_1 F(x_1|\omega) \exp[-iqx_1 - i\alpha_0(q)\zeta(x_1)], \quad (1.2)$$

where the source function  $F(x_1|\omega)$  is

$$F(x_1|\omega) = 2 \left( -\zeta'(x_1) \frac{\partial}{\partial x_1} + \frac{\partial}{\partial x_3} \right) \times E_2(x_1, x_3|\omega)_{inc} \Big|_{x_3=\zeta(x_1)}. \quad (1.3)$$

Substitution of Eq. (1.3) into Eq. (1.2), followed by an integration by parts, yields the result that

$$R(q|k) = \frac{\omega^2/c^2 + \alpha_0(q)\alpha_0(k) - qk}{\alpha_0(q)[\alpha_0(q) + \alpha_0(k)]} \times \int_{-\infty}^{\infty} dx_1 \exp[-i(q-k)x_1 - ia\zeta(x_1)], \quad (1.4)$$

where, to simplify the notation, we have defined  $a = \alpha(q) + \alpha_0(k)$ .

The mean differential reflection coefficient  $\langle \partial R_s / \partial \theta_s \rangle$ , which is defined such that  $\langle \partial R_s / \partial \theta_s \rangle d\theta_s$  gives the fraction of the total, time-averaged, flux incident on the surface that is scattered into the angular interval  $(\theta_s, \theta_s + d\theta_s)$ , is given in terms of  $R(q|k)$  by

$$\left\langle \frac{\partial R_s}{\partial \theta_s} \right\rangle = \frac{1}{L_1} \frac{\omega}{2\pi c} \frac{\cos^2 \theta_s}{\cos \theta_0} \langle |R(q|k)|^2 \rangle, \quad (1.5)$$

where the angle brackets denote an average over the ensemble of realizations of the surface profile function  $\zeta(x_1)$ ,  $\theta_0$  and  $\theta_s$  are the angles of incidence and scattering respectively, which are related to the wave numbers  $k$  and  $q$  by  $k = (\omega/c) \sin \theta_0$  and  $q = (\omega/c) \sin \theta_s$ , and  $L_1$  is the length of the  $x_1$ -axis covered by the random surface.

With the use of Eq. (1.4) the average  $\langle |R(q|k)|^2 \rangle$  entering Eq. (1.5) can be written as

$$\begin{aligned} \langle |R(q|k)|^2 \rangle &= \left[ \frac{1 + \cos(\theta_0 + \theta_s)}{\cos \theta_s (\cos \theta_0 + \cos \theta_s)} \right]^2 \\ &\times \int_{-\infty}^{\infty} dx_1 \int_{-\infty}^{\infty} dx'_1 \exp[-i(q-k)(x_1 - x'_1)] \\ &\times \left\langle \exp[-ia(\zeta(x_1) - \zeta(x'_1))] \right\rangle. \end{aligned} \quad (1.6)$$

We focus on the integral in Eq. (1.6). With the change of variable  $x'_1 = x_1 + u$  it becomes

$$I(q|k) = \int_{-\infty}^{\infty} dx_1 \int_{-\infty}^{\infty} du \exp[i(q-k)u] \times \left\langle \exp[-ia(\zeta(x_1) - \zeta(x_1 + u))] \right\rangle. \quad (1.7)$$

The geometrical optics limit of the Kirchhoff approximation is obtained by expanding the difference  $\zeta(x_1) - \zeta(x_1 + u)$  in Eq. (1.7) in power of  $u$  and retaining only the leading nonzero term:

$$I(q|k) \cong \int_{-\infty}^{\infty} dx_1 \int_{-\infty}^{\infty} du \exp[i(q-k)u] \left\langle \exp[ia u \zeta'(x_1)] \right\rangle. \quad (1.8)$$

Because we have not assumed  $\zeta(x_1)$  to be a stationary random process, we cannot assume that  $\zeta'(x_1)$  is a stationary random process. The average  $\langle \exp[ia u \zeta'(x_1)] \rangle$ , therefore, has to be assumed to be a function of  $x_1$ , and we cannot out the integral over  $x_1$  to yield a factor of  $L_1$ , as we could if  $\zeta(x_1)$  were a stationary random process.

## 2. Design of a Band-Limited Uniform Diffuser

To evaluate the average in Eq. (1.8) we begin by writing the surface profile function  $\zeta(x_1)$  in the form

$$\zeta(x_1) = \sum_{l=-\infty}^{\infty} c_l s(x_1 - 2lb), \quad (2.1)$$

where the  $\{c_l\}$  are independent, positive, random deviates. These properties of the  $\{c_l\}$  are dictated by the fabrication process, described in Section 4. The function  $s(x_1)$  is defined by

$$\begin{aligned} s(x_1) &= 0, & x_1 < -(m+1)b, \\ &= -(m+1)bh - hx_1, & -(m+1)b < x_1 < -mb, \\ &= -bh, & -mb < x_1 < mb, \\ &= -(m+1)bh + hx_1, & mb < x_1 < (m+1)b, \\ &= 0, & (m+1)b < x_1, \end{aligned} \quad (2.2)$$

where  $m$  is a positive integer and  $b$  is a characteristic length.

The derivative of the surface profile function,  $\zeta'(x_1)$ , is then given by

$$\zeta'(x_1) = \sum_{l=-\infty}^{\infty} c_l d(x_1 - 2lb), \quad (2.3)$$

where

$$\begin{aligned} d(x_1) &= 0, & x_1 < -(m+1)b, \\ &= -h, & -(m+1)b < x_1 < -mb, \\ &= 0, & -mb < x_1 < mb, \\ &= h, & mb < x_1 < (m+1)b, \\ &= 0, & (m+1)b < x_1. \end{aligned} \quad (2.4)$$

The function  $s(x_1)$  and  $d(x_1)$  are shown in Fig. 1.

In what follows the surface will be sampled at the set of equally spaced points  $\{x_p\}$  defined by

$$x_p = \left(p + \frac{1}{2}\right) b/N \quad p = 0, \pm 1, \pm 2, \dots, \quad (2.5)$$

where  $N$  is a large positive integer. None of these values of  $x_p$  equals an integer multiple of  $b$ , at which  $d(x_1)$  is discontinuous.

When the probability density function (pdf) of  $c_l$ ,

$$f(\gamma) = \langle \delta(\gamma - c_l) \rangle, \quad (2.6)$$

is known, a long sequence of the  $\{c_l\}$  can be generated, e.g. by the rejection method [7], from which the surface profile function  $\zeta(x_1)$  can be obtained by the use of Eqs. (2.1) and (2.2). We note that since the  $\{c_l\}$  are positive random deviates,  $f(\gamma)$  will be nonzero only for positive values of  $\gamma$ .

The average  $\langle \exp iau \zeta'(x_1) \rangle$  can now be written as

$$\begin{aligned} \langle \exp iau \zeta'(x_1) \rangle &= \left\langle \exp \left\{ iau \sum_{l=-\infty}^{\infty} c_l d(x_1 - 2lb) \right\} \right\rangle \\ &= \left\langle \prod_{l=-\infty}^{\infty} \exp \{ iau c_l d(x_1 - 2lb) \} \right\rangle \\ &= \prod_{l=-\infty}^{\infty} \left\langle \exp \{ iau c_l d(x_1 - 2lb) \} \right\rangle, \end{aligned} \quad (2.7)$$

where the independence of the  $\{c_l\}$  has been used in the last step. With the form of  $d(x_1)$  given by Eq. (2.4), for any value of  $x_1$  chosen from the set of sampling points  $\{x_p\}$  given by Eq. (2.5) only one factor in the infinite product on the right hand side of Eq. (2.7) is different from unity. Indeed, we find for  $m = 2$  that when  $2nb < x_1 < (2n+1)b$  ( $n = 0, \pm 1, \pm 2, \dots$ )

$$\begin{aligned} \langle \exp iau \zeta'(x_1) \rangle &= \langle \exp \{ iauhc_{n-1} \} \rangle \\ &= \int_{-\infty}^{\infty} d\gamma f(\gamma) \exp(iauh\gamma), \end{aligned} \quad (2.8a)$$

while when  $(2n-1)b < x_1 < 2nb$  ( $n = 0, \pm 1, \pm 2, \dots$ )

$$\begin{aligned} \langle \exp iau \zeta'(x_1) \rangle &= \langle \exp \{ -iauhc_{n+1} \} \rangle \\ &= \int_{-\infty}^{\infty} d\gamma f(\gamma) \exp(-iauh\gamma). \end{aligned} \quad (2.8b)$$

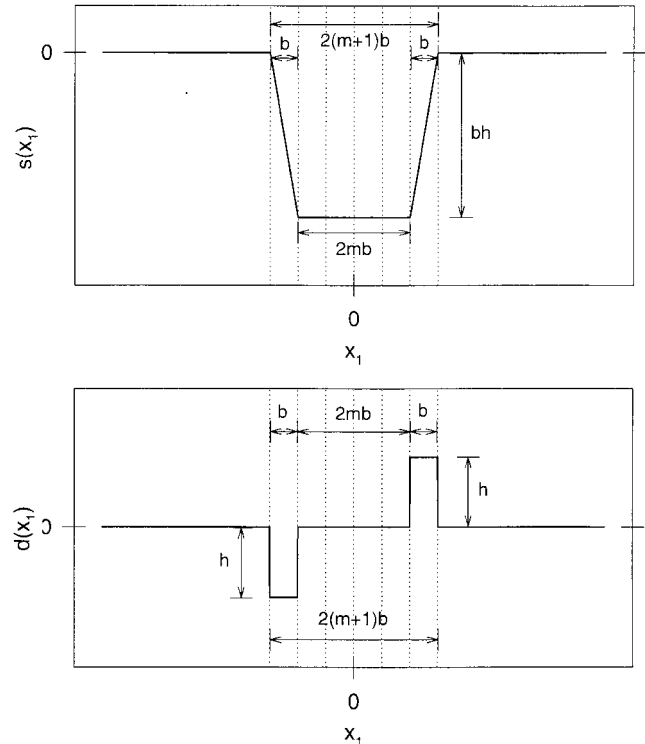


Figure 1. The functions  $s(x_1)$  and  $d(x_1)$ .

When the results given by Eqs. (2.8) are substituted into Eq. (1.8), the latter becomes

$$\begin{aligned} I(q|k) &= \sum_n \int_{2nb}^{(2n+1)b} dx_1 \int_{-\infty}^{\infty} du \exp[i(q-k)u] \\ &\quad \times \int_{-\infty}^{\infty} d\gamma f(\gamma) \exp(ia\gamma hu) \\ &\quad + \sum_n \int_{(2n-1)b}^{2nb} \int_{-\infty}^{\infty} du \exp[i(q-k)u] \\ &\quad \times \int_{-\infty}^{\infty} d\gamma f(\gamma) \exp(-ia\gamma hu) \\ &= \frac{L_1}{2} \int_{-\infty}^{\infty} du \exp[i(q-k)u] \\ &\quad \times \int_{-\infty}^{\infty} d\gamma f(\gamma) \left[ \exp(ia\gamma hu) + \exp(-ia\gamma hu) \right] \\ &= \pi L_1 \int_{-\infty}^{\infty} d\gamma f(\gamma) \left[ \delta(q-k+ah\gamma) + \delta(q-k-ah\gamma) \right] \\ &= \frac{\pi L_1}{ah} \left[ f\left(\frac{k-q}{ah}\right) + f\left(\frac{q-k}{ah}\right) \right]. \end{aligned} \quad (2.9)$$

We note that although Eqs. (2.8) were obtained for the case that  $m = 2$ , the result given by Eq. (2.9) is valid for any  $m$ .

When the results given by Eqs. (1.7), (1.8) and (2.9) are substituted into Eq. (2.6), we find that the mean differential reflection coefficient is given by

$$\begin{aligned} \left\langle \frac{\partial R_s}{\partial \theta_s} \right\rangle &= \frac{1}{2h} \frac{[1 + \cos(\theta_0 + \theta_s)]^2}{\cos \theta_0 (\cos \theta_0 + \cos \theta_s)^3} \\ &\times \left[ f \left( \frac{\sin \theta_0 - \sin \theta_s}{h(\cos \theta_0 + \cos \theta_s)} \right) \right. \\ &\left. + f \left( \frac{\sin \theta_s - \sin \theta_0}{h(\cos \theta_0 + \cos \theta_s)} \right) \right]. \end{aligned} \quad (2.10)$$

Thus, we find that in the geometrical optics limit of the Kirchhoff approximation the mean differential reflection coefficient is determined by the pdf  $f(\gamma)$  of the coefficient  $c_l$  entering the expansions (2.1) and (2.3). We also note that it is independent of the wavelength of the incident light.

The result given by Eq. (2.10) simplifies significantly in the case of normal incidence,  $\theta_0 = 0^\circ$ :

$$\begin{aligned} \left\langle \frac{\partial R_s}{\partial \theta_s} \right\rangle &= \left( 1 + \tan^2 \frac{\theta_s}{2} \right) \\ &\times \frac{f \left( -\frac{1}{h} \tan \frac{\theta_s}{2} \right) + f \left( \frac{1}{h} \tan \frac{\theta_s}{2} \right)}{4h}. \end{aligned} \quad (2.11)$$

The mean differential reflection coefficient given by this result is normalized to unity,

$$\int_{-\pi/2}^{\pi/2} d\theta_s \left\langle \frac{\partial R_s}{\partial \theta_s} \right\rangle = 1. \quad (2.12)$$

From the result given by Eq. (2.11) we find that if we wish a constant value for  $\langle \partial R / \partial \theta_s \rangle$  for  $-\theta_m < \theta_s < \theta_m$ , we must choose

$$f(\gamma) = \frac{h}{\tan^{-1} \gamma_m h} \frac{\theta(\gamma)\theta(\gamma_m - \gamma)}{1 + \gamma^2 h^2}, \quad (2.13)$$

where  $\gamma_m = [\tan(\theta_m/2)]/h$ , because in this case

$$\left\langle \frac{\partial R_s}{\partial \theta_s} \right\rangle = \frac{\theta(\theta_m - |\theta_s|)}{2\theta_m}. \quad (2.14)$$

It is worth noting that if the maximum scattering angle  $\theta_m = 2 \tan^{-1}(h\gamma_m)$  is small enough, e.g.  $\theta_m = 20^\circ$ , so that  $\gamma_m h = 0.1763$ , with little error we can neglect  $\gamma^2 h^2$  compared to unity in the denominator on the right hand side of Eq. (2.13) ( $\gamma^2 h^2 < \gamma_m^2 h^2 = 0.0311$ ), and can replace  $\tan^{-1} \gamma_m h$  by  $\gamma_m h$  as well ( $\tan^{-1} \gamma_m h = 0.1745$ ), to obtain for  $f(\gamma)$  the simple form

$$f(\gamma) \cong \theta(\gamma)\theta(\gamma_m - \gamma)/\gamma_m. \quad (2.15)$$

If the required maximum scattering angle is not small, one has to use the result given by Eq. (2.13) for  $f(\gamma)$ .

### 3. Computer Simulations

The approach to the design of band-limited uniform diffusers presented in the preceding sections was tested by means of computer simulation calculations. One-dimensional random surfaces were generated numerically on the basis of Eqs. (2.1) and (2.2) with the coefficients  $\{c_l\}$  determined by the rejection method with the use of the pdf (2.15). As an example, we show in Fig. 2 a realization of a sample profile and its derivative, generated in this way.

For a given surface profile the scattering amplitude  $R(q|k)$  can be calculated in the Kirchhoff approximation, but without passing to the geometrical optics limit, from Eq. (1.4). The mean differential reflection coefficient can then be calculated from Eq. (1.5) by generating a large number  $N_p$  of surface profiles and averaging over the resulting scattering distributions. In Fig. 3 we show an example of a calculated mean differential reflection coefficient obtained by averaging results obtained for 3000 realizations of the surface profile function. It is seen that the scattering distribution is close to the desired result. There is almost no light outside the range  $-\theta_m < \theta_s < \theta_m$  and, apart from a small peak in the specular direction, the distribution is fairly uniform. This peak is part of the diffuse component of the scattered light, as the specular component is negligible in this case. It is due to the fact that our analysis is based on the geometrical optics approximation, and it is worth discussing this point in more detail.

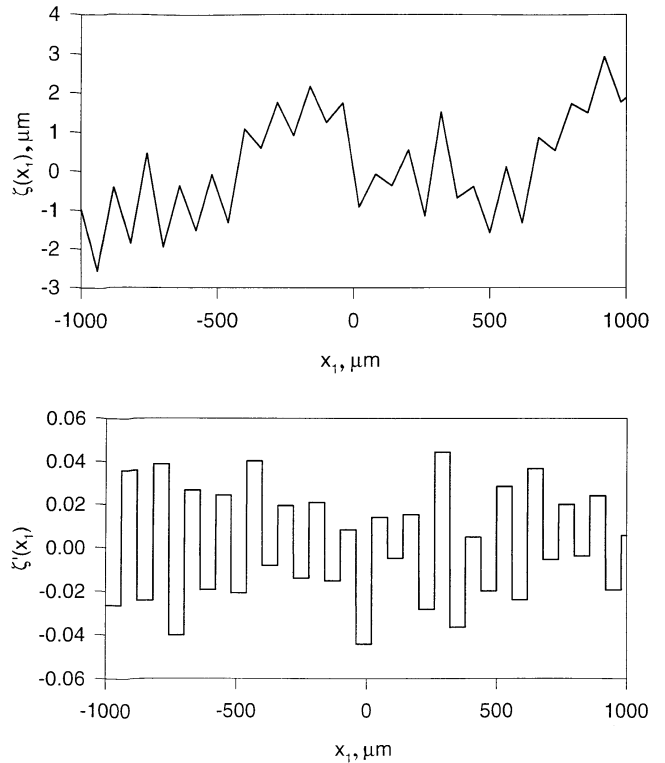


**Figure 2.** Numerical generation of a surface profile and its derivative. The parameters employed are  $b = 60 \mu\text{m}$ ,  $m = 1$ ,  $\gamma_m = 1$  and  $\theta_m = 5^\circ$ .

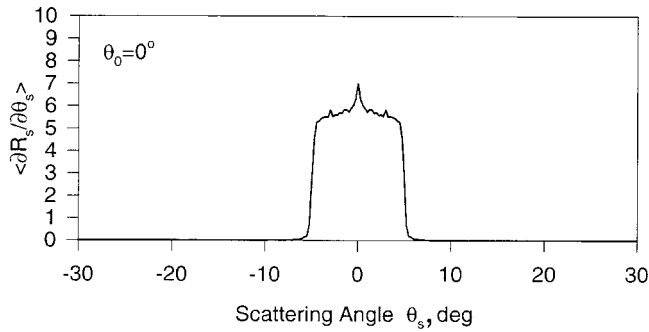


**Figure 3.** The mean differential reflection coefficient for normal incidence calculated from  $N_p = 3000$  realizations of the surface profile function. The parameters employed are  $\lambda = 0.6328 \mu\text{m}$ ,  $b = 60 \mu\text{m}$ ,  $m = 1$ ,  $\gamma_m = 1$ , and  $\theta_m = 5^\circ$ . The sampling interval on the surface was  $\Delta x = b/N = 0.2 \mu\text{m}$  ( $N = 300$ ), and the length of the surface was  $L_1 = 2000 \mu\text{m}$ .

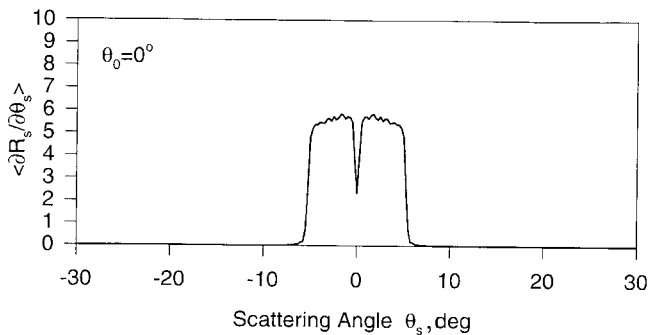


**Figure 4.** The same as Fig. 3, but with random deviates  $\{c_l\}$  drawn from the distribution given by Eq. (3.1) with  $\varepsilon = 0.05$ .

We see from Eqs. (2.11) and (2.15) that in the geometrical optics limit of the Kirchhoff approximation the scattering distribution consists of two rectangular distributions, and it is clear that diffraction effects will smooth these two contributions. The peak observed in the specular direction in the scattering distribution plotted in Fig. 3 is due to the overlap of the tails of the two distributions predicted on the basis of the geometrical optics approximation. To illustrate this point we present, in Fig. 4, a mean differential reflection coefficient for the case in which the random numbers are generated from a drc of the form

$$f(\gamma) = \theta(\gamma - \varepsilon)\theta(\gamma_m + \varepsilon - \gamma)/\gamma_m, \quad (3.1)$$

where  $\varepsilon = 0.05$ . In our approximation the scattering distribution is then given by

$$\begin{aligned} \left\langle \frac{\partial R_s}{\partial \theta_s} \right\rangle \cong & \frac{1}{4\gamma_m h} \left[ \theta \left( -\frac{\theta_s}{2h} - \varepsilon \right) \theta \left( \gamma_m + \varepsilon + \frac{\theta_s}{2h} \right) \right. \\ & \left. + \theta \left( \frac{\theta_s}{2h} - \varepsilon \right) \theta \left( \gamma_m + \varepsilon - \frac{\theta_s}{2h} \right) \right], \quad (3.2) \end{aligned}$$

where the smallness of  $\theta_m$  has been used in obtaining this result. It can be seen that this distribution agrees well with

the result shown in Fig. 4, the main difference being that in the numerical results the two sections of the scattering distribution are not completely separated due to the overlap of their tails, which give rise to a dip in  $\langle \partial R_s / \partial \theta_s \rangle$ . Thus, a value of  $\varepsilon$  intermediate between 0 and 0.5 should yield an approximately flat scattering curve. That this is the case is shown in Fig. 5, where  $\langle \partial R_s / \partial \theta_s \rangle$  is plotted for a surface the basis of the pdf (3.1) with  $\varepsilon = 0.01$ , and for the same values of  $\theta_0$ ,  $b$ ,  $m$ ,  $\gamma_m$ , and  $\theta_m$  used in obtaining Figs. 3 and 4. Results are presented for three wavelengths of the incident light: *a* —  $\lambda = 0.6328 \mu\text{m}$  (He-Ne laser); *b* —  $\lambda = 0.532 \mu\text{m}$  (the second harmonic of the YAG laser); *c* —  $\lambda = 0.442 \mu\text{m}$  (He-Cd laser). These wavelengths cover the entire visible region of the optical spectrum. For each wavelength the result for  $\langle \partial R_s / \partial \theta_s \rangle$  is seen to consist of a nearly constant scattered intensity for  $\theta_s$  between  $-5^\circ$  and  $+5^\circ$ , and a zero scattered intensity outside this interval. Moreover, these results confirm the expected independence of the scattering pattern from the wavelength of the incident light over a significant range of wavelengths.

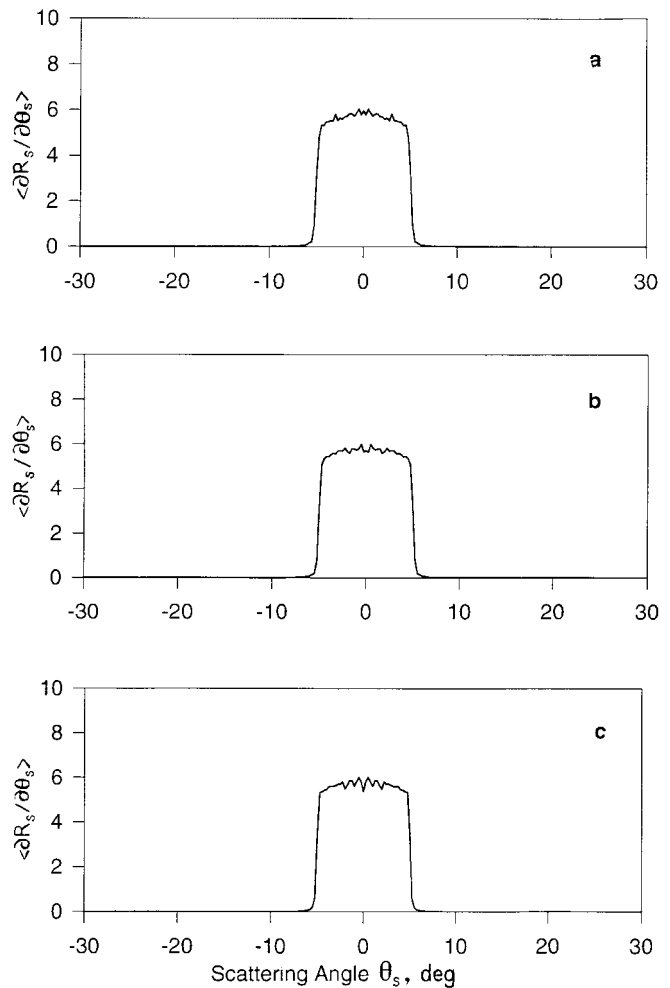


**Figure 5.** The same as Fig. 4, but with  $\varepsilon = 0.01$ . *a* —  $\lambda = 0.6328 \mu\text{m}$ ; *b* —  $\lambda = 0.532 \mu\text{m}$ ; *c* —  $\lambda = 0.442 \mu\text{m}$ .

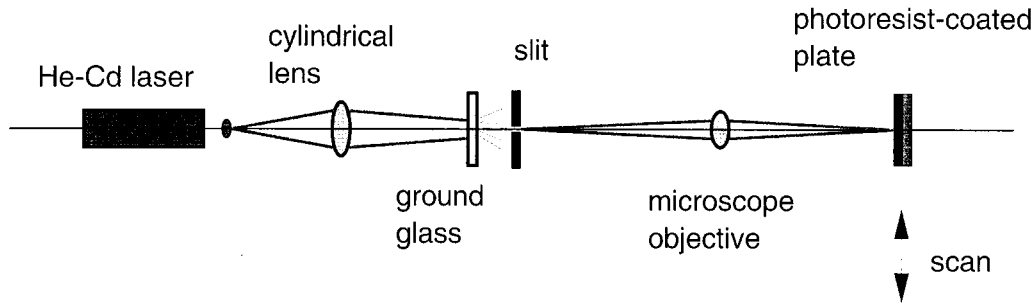


Figure 6. Schematic diagram of the experimental arrangement employed for the fabrication of the diffusers.

### 4. Experimental Results

A schematic diagram of the optical system used in our efforts to fabricate the kind of surface studied in this paper is shown in Fig. 6. The illumination is provided by a He–Cd laser (wavelength  $\lambda = 442 \text{ nm}$ ). An optical system concentrates the light transmitted through a rotating ground glass on a slit, providing illumination that is effectively incoherent. An incoherent image of the slit is formed by an X1 (numerical aperture 0.05) microscope objective on a photoresist-coated glass plate.

The width of the slit is approximately  $l = 180 \mu\text{m}$ , and its incoherent image has a nearly rectangular shape (smoothed by diffraction). In order to fabricate grooves with the desired trapezoidal shape on the photoresist, the plate is exposed while executing a scan of length  $b = l/(2m + 1)$ . This procedure generates, basically, a function  $s(x_1)$  with the shape defined by Eq. (2.2). The depth of the groove is determined by the time of exposure. An example of such a fabricated groove is shown in Fig. 7, which presents the measured surface profile of a section of a photoresist plate that was exposed in this fashion. Although the corners are not as sharp as the ones in Fig. 1, *a*, the result approximates the desired shape quite well.

The photoresist plate is exposed to grooves generated in this fashion, with random depths and displaced sequentially in steps of  $2b$ . Several hundred uncorrelated random numbers  $\{c_i\}$  are generated in the computer with the specified  $f(\gamma)$ . At each position  $x_1 = 2bl$ , The time of exposure of the groove is proportional to the random number  $c_i$  generated in the computer [8].

In Fig. 8 we present a profilometric trace of one of the samples fabricated according to Eq. (2.1). The faceted nature of the surface is clearly visible in the figure. In the example displayed we chose  $m = 0$ , which produces a function  $s(x_1)$  of triangular rather than trapezoidal form. The resulting symmetric triangular indentations are clearly visible in the figure. Thus, these preliminary results indicate that the proposed fabrication method is able to produce random uniform diffusers.

In order to study experimentally the scattering properties of these photoresist diffusers in reflection they would have had to be coated with a thin metallic layer. Instead,

we studied these properties in the simpler case of the transmission of *s*-polarized light through them. Although the theoretical work motivating the method for fabricating the uniform diffusers described in the preceding sections was based on reflection, an analysis carried out within the framework of the geometrical optics limit of the thin phase screen model [9] shows that surfaces that act as band-limited uniform diffusers in reflection also act as uniform band-limited diffusers in transmission, although the

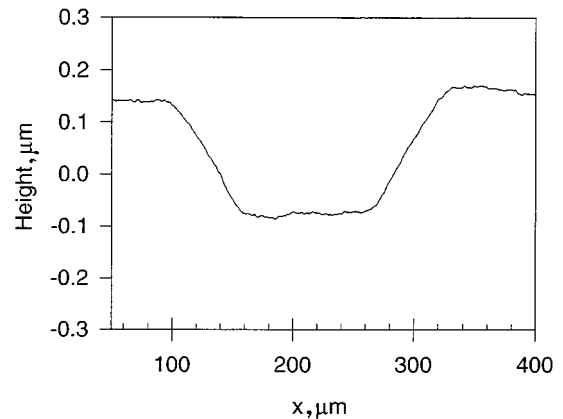


Figure 7. Measured profile that illustrates the experimental realization of the function  $s(x_1)$ . The profile was measured by means of a Dektak<sup>(st)</sup> mechanical profilometer.

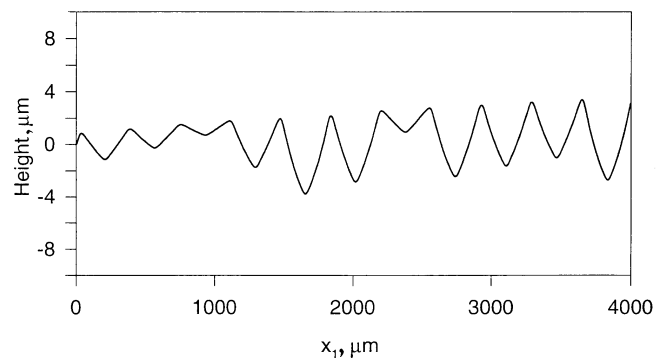
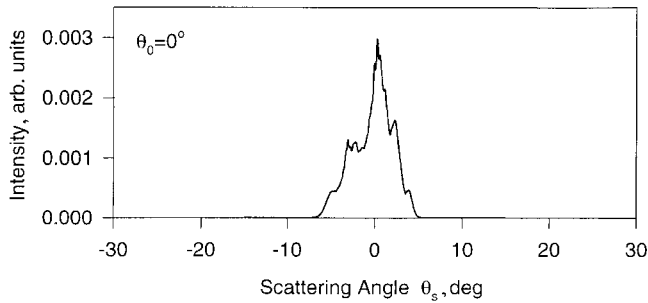


Figure 8. Measured segment of a surface profile for a fabricated sample. The parameters are  $b = 60 \mu\text{m}$ ,  $m = 0$ .



**Figure 9.** Experimental result for the angular dependence of the intensity of  $s$ -polarized light of wavelength  $\lambda = 0.6328 \mu\text{m}$  transmitted through a photoresist film. The angle of incidence is  $\theta_0 = 0^\circ$ . The illuminated surface of the film is a one-dimensional random surface through which light is transmitted within the angle  $-5^\circ < \theta_s < 5^\circ$ , and is not transmitted outside this range.

maximum scattering angle  $\theta_m$  in transmission is different that it is in reflection [10]. However, the transmission patterns obtained with the diffusers fabricated up to now, although band-limited, are not uniform (Fig. 9). Large intensity fluctuations are present in the angular region in which a constant intensity would be expected. The origin of these fluctuations is the small number of randomly oriented facets that are etched in our surfaces. They represent, simply, statistical noise. For the lengths of the surfaces that we have fabricated only about two hundred random numbers  $c_l$  are employed. Efforts are currently underway to fabricate surfaces with a larger number of randomly oriented facets.

## 5. Summary and Conclusions

In this paper we have described approaches to designing and fabricating one-dimensional, random, band-limited, uniform diffusers. These approaches are well suited for the generation of such surfaces on photoresist. The results of computer simulations, and some preliminary experimental results, indicate that uniform band-limited diffusers can be fabricated by the method proposed.

The design of band-limited uniform diffusers is but one interesting inverse problem involving the design of random surfaces with specified scattering properties. The design of a Lambertian diffuser, namely a random surface that produces a scattered intensity proportional to the cosine of the polar scattering angle, is another [11]. Finally, the design and fabrication of two-dimensional random surfaces with specified light scattering properties pose interesting theoretical and experimental challenges. Some first steps in this direction have been taken recently [12], but more remains to be done.

This paper is dedicated to the A.F. Ioffe Physico-technical institute on the occasion of its 80th anniversary, with best wishes for many more years of significant contributions to science. The work reported here was supported in part by Army Research Office grants DAAH 04-96-1-0187 and DAAG 55-98-C-0034.

## References

- [1] L.I. Mandel'shtam. *Ann. Physik* **41**, 609 (1913).
- [2] C.N. Kurtz. *J. Opt. Soc.* **62**, 929 (1972).
- [3] C.N. Kurtz, H.O. Hoadley, J.J. DePalma. *J. Opt. Soc. Am.* **63**, 1080 (1973).
- [4] Y. Nakayama, M. Kato. *Appl. Opt.* **21**, 1410 (1982).
- [5] M. Kowalczyk. *Opt. Soc. Am.* **A1**, 192 (1984).
- [6] E.R. Méndez, G. Martínez-Niconoff, A.A. Maradudin, T.A. Leskova. *SPIE* **3426** (1998), to appear.
- [7] W.H. Press, S.A. Teukolsky, W.T. Vetterling, B.P. Flannery. *Numerical Recipes, in Fortran. 2nd Edition.* Cambridge University Press, N.Y. (1992). P. 281.
- [8] E.R. Méndez, M.A. Ponce, V. Ruiz-Cortés, Zu-Han Gu. *Appl. Opt.* **30**, 4103 (1991).
- [9] W.T. Welford. *Opt. Quant. Electron.* **9**, 269 (1977).
- [10] T.A. Leskova, A.A. Maradudin, I.V. Novikov, A.V. Schchegrov, E.R. Méndez. University of California, Irvine, Department of Physics and Astronomy, Technical Report N 98-2 (1998).
- [11] H.P. Balthes. In: *Inverse Scattering Problems in Optics / Ed. by H.P. Balthes.* Springer-Verlag, N.Y. (1998). P. 1.
- [12] E.R. Méndez, G. Marínez-Niconoff, A.A. Maradudin, T.A. Leskova. *Proc. Reunion Iberoamericana de Optica.* Cartagena, Columbia (1998), to appear.